\# 3864

47

Trans. SHASE
No. 24, Feb., 1984

Evaluation of Ventilation Systems through Numerical Computation and Presentation of a New Ventilation Model*1

by Yoshiaki ISHIZU*2 and Kazuyo KANEKI*3

Synopsis: The efficiency of various types of ventilation systems is examined by numerical calculation for two-dimensional, isothermal, and turbulent flow models. It is found that the ventilation is effective when the main pass length of the supplied air flow in a room is long. Since the slope of the concentration decay seems to become virtually constant and independent of the position in the room, this slope is proposed as a criterion for the ventilation efficiency. Further, a new convenient ventilation model is presented with the introduction of two parameters showing the ventilation efficiency and the effect of the pollutant generation site.

Introduction

As buildings are becoming larger and more airtight, people are spending a lot of time in an artificial environment. Therefore, besides conventional air conditioning for temperature and humidity, the cleanliness of the room air should be guaranteed for the health of the occupants.

Theoretically, the cleanliness of the air can be ensured by increasing the ventilation rate. However, this method opposes the energy-saving requirements. Thus, the development of an optimum, or effective, ventilation system compatible with these contradictory requisites is desirable.

Fortunately, turbulent flow models for numerical calculation have been improved remarkably in the past decade, and the k-ε model, in particular, is becoming a powerful model for the prediction of flow characteristics[1),2)].

This paper describes the evaluation of the efficiency of various ventilation systems from the results of numerical calculation for two-dimensional, isothermal, and turbulent flows. Further, a new ventilation model for the expression of the average pollutant concentration is proposed with the introduction of two factors showing the ventilation efficiency and the effect of the pollutant generation site.

1. Nomenclature

C : Concentration

C_0 : Initial concentration of pollutant in room

C_e : Concentration of pollutant in exhaust air

C_i : Concentration of pollutant in outdoor air

C_∞ : Steady state concentration of pollutant in room

D : Effective turbulent diffusion coefficient

G : Pollutant generation rate

---

*1 A part of this paper was presented at the 4th International Symposium on the Use of Computers for Environmental Engineering related to Buildings held in Tokyo, Japan, March 1983.

*2 Central Research Institute, The Japan Tobacco and Salt Public Corporation, Member

*3 Central Research Institute, The Japan Tobacco and Salt Public Corporation

k : Turbulence kinetic energy
l_0 : Width of inlet
m : Mixing factor
n : Normal distance
p : Position factor
Q : Air flow rate
t : Time
u, v : Mean component of velocity in direction x and y
v_0 : Flow velocity at inlet
V : Volume of room
x, y : Cartesian space coordinate

Greek Symbols

Γ_k : Effective turbulent diffusion coefficient for diffusion of $k(=\nu_0+\Gamma_{k,t})$
$\Gamma_{k,t}$: Turbulent diffusion coefficient for diffusion of $k(=\nu_t/\sigma_k)$
Γ_ε : Effective turbulent diffusion coefficient for diffusion of $\varepsilon(=\nu_0+\Gamma_{\varepsilon,t})$
$\Gamma_{\varepsilon,t}$: Turbulent diffusion coefficient for diffusion of $\varepsilon(=\nu_t/\sigma_\varepsilon)$
ε : Turbulence energy dissipation rate
ν : Effective turbulent kinematic viscosity $(=\nu_0+\nu_t)$
ν_0 : Kinematic viscosity
ν_t : Turbulent kinematic viscosity
$\sigma_1, \sigma_2, \sigma_\mu$: Coefficients in approximated turbulent transport equations
$\sigma_k, \sigma_\varepsilon, \sigma_C$: Turbulent Schmidt number corresponding to k, ε, C
ϕ : Generalized dependent variable
ψ : Stream function
ω : Vorticity

Subscript

α : Generalized subscript
w : Wall
1 : Zone 1 of the room
2 : Zone 2 of the room
b : By-pass

2. Basic Equations[3)]

2.1 Steady State

The basic equations are:

1) Stream function equation

$$\frac{\partial^2\psi}{\partial x^2}+\frac{\partial^2\psi}{\partial y^2}=-\omega \qquad \cdots\cdots(1)$$

2) Vorticity equation

$$\frac{\partial}{\partial x}\left(\omega\frac{\partial\psi}{\partial y}\right)-\frac{\partial}{\partial y}\left(\omega\frac{\partial\psi}{\partial x}\right)$$
$$=\frac{\partial^2}{\partial x^2}(\nu\omega)+\frac{\partial^2}{\partial y^2}(\nu\omega)-4\frac{\partial^2\psi}{\partial x\partial y}\frac{\partial^2\nu}{\partial x\partial y}$$
$$+2\frac{\partial^2\psi}{\partial y^2}\frac{\partial^2\nu}{\partial x^2}+2\frac{\partial^2\psi}{\partial x^2}\frac{\partial^2\nu}{\partial y^2} \qquad \cdots\cdots(2)$$

3) k-equation

$$\frac{\partial}{\partial x}\left(k\frac{\partial\psi}{\partial y}\right)-\frac{\partial}{\partial y}\left(k\frac{\partial\psi}{\partial x}\right)$$
$$=\frac{\partial}{\partial x}\left(\Gamma_k\frac{\partial k}{\partial x}\right)+\frac{\partial}{\partial y}\left(\Gamma_k\frac{\partial k}{\partial y}\right)$$
$$+\nu_t\left\{4\left(\frac{\partial^2\psi}{\partial x\partial y}\right)^2+\left(\frac{\partial^2\psi}{\partial y^2}-\frac{\partial^2\psi}{\partial x^2}\right)^2\right\}-\frac{\sigma_\mu k^2}{\nu_t} \qquad \cdots\cdots(3)$$

4) ε-equation

$$\frac{\partial}{\partial x}\left(\varepsilon\frac{\partial\psi}{\partial y}\right)-\frac{\partial}{\partial y}\left(\varepsilon\frac{\partial\psi}{\partial x}\right)$$
$$=\frac{\partial}{\partial x}\left(\Gamma_\varepsilon\frac{\partial\varepsilon}{\partial x}\right)+\frac{\partial}{\partial y}\left(\Gamma_\varepsilon\frac{\partial\varepsilon}{\partial y}\right)$$
$$+\sigma_1\sigma_\mu k\left\{4\left(\frac{\partial^2\psi}{\partial x\partial y}\right)^2+\left(\frac{\partial^2\psi}{\partial y^2}-\frac{\partial^2\psi}{\partial x^2}\right)^2\right\}-\frac{\sigma_2\varepsilon^2}{k} \qquad \cdots\cdots(4)$$

5) Concentration equation

$$\frac{\partial}{\partial x}\left(C\frac{\partial\psi}{\partial y}\right)-\frac{\partial}{\partial y}\left(C\frac{\partial\psi}{\partial x}\right)$$
$$=\frac{\partial}{\partial x}\left(D\frac{\partial C}{\partial x}\right)+\frac{\partial}{\partial y}\left(D\frac{\partial C}{\partial y}\right)+G \qquad \cdots\cdots(5)$$

where,

ψ : Stream function
ω : Vorticity
k : Turbulence kinetic energy
ε : Turbulence energy dissipation rate
C : Concentration
$\nu_t=\sigma_\mu k^2/\varepsilon$
$\nu=1/Re+\nu_t$
$\Gamma_k=1/Re+\nu_t/\sigma_k$
$\Gamma_\varepsilon=1/Re+\nu_t/\sigma_\varepsilon$
$D=1/(ReSc)+\nu_t/\sigma_c$

All of the parameters have been made nondimensional, with the characteristic length being the width of the inlet, l_0, the characteristic velocity being the flow rate at the inlet, v_0, and the characteristic concentration being $1/l_0^2$.

2.2 Unsteady State

Only the case when the concentration changes with time while the flow remains steady is considered as the unsteady state. Accordingly, the basic equations differ from those of the steady

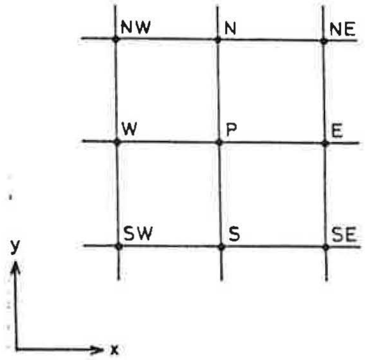

Fig. 1 Arrangement of the subscripts

state in the concentration equation as follows:

5′) Concentration equation

$$\frac{\partial C}{\partial t}+\frac{\partial}{\partial x}\left(C\frac{\partial \psi}{\partial y}\right)-\frac{\partial}{\partial y}\left(C\frac{\partial \psi}{\partial x}\right)$$
$$=\frac{\partial}{\partial x}\left(D\frac{\partial C}{\partial x}\right)+\frac{\partial}{\partial y}\left(D\frac{\partial C}{\partial y}\right)+G \qquad \cdots\cdots(6)$$

3. Finite Difference Approximation

The basic equations are solved numerically by the following finite difference approximation[8]. The relation among the subscripts is shown in **Figure 1.**

3.1 Steady State

1) Stream function equation

$$\psi_p=(\psi_E+\psi_W+\psi_N+\psi_S+\omega_p d_p)/4 \qquad \cdots\cdots(7)$$

2) Vorticity equation

$$\omega_p=\{(b_E+\nu_E)\omega_E+(b_W+\nu_W)\omega_W+(b_N+\nu_N)\omega_N$$
$$+(b_S+\nu_S)\omega_S-S_{\omega p}d_p\}/(\Sigma b+4\nu_p) \qquad \cdots\cdots(8)$$

3) k-equation

$$k_p=\{(b_E+A_E{}^k)k_E+(b_W+A_W{}^k)k_W$$
$$+(b_N+A_N{}^k)k_N+(b_S+A_S{}^k)k_S$$
$$+S_{kp}d_p\}/(\Sigma b+\Sigma A^k+\sigma_\mu k_p d_p/\nu_{t,p}) \qquad \cdots\cdots(9)$$

4) ε-equation

$$\varepsilon_p=\{(b_E+A_E{}^\varepsilon)\varepsilon_E+(b_W+A_W{}^\varepsilon)\varepsilon_W+(b_N+A_N{}^\varepsilon)\varepsilon_N$$
$$+(b_S+A_S{}^\varepsilon)\varepsilon_S+S_{\varepsilon p}d_p\}/(\Sigma b+\Sigma A^\varepsilon+\sigma_2\varepsilon_p d_p/k_p)$$
$$\cdots\cdots(10)$$

5) Concentration equation

$$C_p=\{(b_E+A_E{}^C)C_E+(b_W+A_W{}^C)C_W$$
$$+(b_N+A_N{}^C)C_N+(b_S+A_S{}^C)C_S$$
$$+G_p d_p\}/(\Sigma b+\Sigma A^C) \qquad \cdots\cdots(11)$$

where,

$$d_p=\Delta x\Delta y$$
$$b_E=\{(\psi_{SE}+\psi_S-\psi_{NE}-\psi_N)+|\psi_{SE}+\psi_S-\psi_{NE}-\psi_N|\}/8$$
$$b_W=\{(\psi_{NW}+\psi_N-\psi_{SW}-\psi_S)+|\psi_{NW}+\psi_N-\psi_{SW}-\psi_S|\}/8$$
$$b_N=\{(\psi_{NE}+\psi_E-\psi_{NW}-\psi_W)+|\psi_{NE}+\psi_E-\psi_{NW}-\psi_W|\}/8$$
$$b_S=\{(\psi_{SW}+\psi_W-\psi_{SE}-\psi_E)+|\psi_{SW}+\psi_W-\psi_{SE}-\psi_E|\}/8$$
$$\Sigma b=b_E+b_W+b_N+b_S$$
$$A_\alpha{}^k=(\Gamma_{k,\alpha}+\Gamma_{k,p})/2 \quad ; \quad \alpha=E,W,N,S$$
$$\Sigma A^k=A_E{}^k+A_W{}^k+A_N{}^k+A_S{}^k$$
$$A_\alpha{}^\varepsilon=(\Gamma_{\varepsilon,\alpha}+\Gamma_{\varepsilon,p})/2 \quad ; \quad \alpha=E,W,N,S$$
$$\Sigma A^\varepsilon=A_E{}^\varepsilon+A_W{}^\varepsilon+A_N{}^\varepsilon+A_S{}^\varepsilon$$
$$A_\alpha{}^C=(D_\alpha+D_p)/2 \quad ; \quad \alpha=E,W,N,S$$
$$\Sigma A^C=A_E{}^C+A_W{}^C+A_N{}^C+A_S{}^C$$
$$S_{\omega p}=-4d_{xy}{}^\psi d_{xy}{}^\nu+2(d_{yy}{}^\psi d_{xx}{}^\nu+d_{xx}{}^\psi d_{yy}{}^\nu)$$
$$S_{kp}=\nu_{t,p}\{4(d_{xy}{}^\psi)^2+(d_{yy}{}^\psi-d_{xx}{}^\psi)^2\}$$
$$S_{\varepsilon p}=\sigma_1\sigma_2 k_p\{4(d_{xy}{}^\psi)^2+(d_{yy}{}^\psi-d_{xx}{}^\psi)^2\}$$
$$d_{xy}{}^\psi=(\psi_{NE}-\psi_{NW}-\psi_{SE}+\psi_{SW})/(4d_p)$$
$$d_{xy}{}^\nu=(\nu_{NE}-\nu_{NW}-\nu_{SE}+\nu_{SW})/(4d_p)$$
$$d_{xx}{}^\psi=(\psi_E+\psi_W-2\psi_p)/(\Delta x)^2$$
$$d_{yy}{}^\psi=(\psi_N+\psi_S-2\psi_p)/(\Delta y)^2$$
$$\nu_{t,p}=\sigma_\mu k_p{}^2/\varepsilon_p=\nu_p-1/Re$$

3.2 Unsteady State

The change in concentration with time was calculated by the commonly used alternating direction implicit method (ADI method).

For the first half of time step Δt, the following equation was applied.

$$\{(\Sigma b+\Sigma A^C)+2\Delta x\Delta y/\Delta t\}C_p{}^{N+1/2}$$
$$=(b_E+A_E{}^C)C_E{}^{N+1/2}+(b_W+A_W{}^C)C_W{}^{N+1/2}$$
$$+(b_N+A_N{}^C)C_N{}^N+(b_S+A_S{}^C)C_S{}^N$$
$$+G_p\Delta x\Delta y+2\Delta x\Delta y C_p{}^N/\Delta t \qquad \cdots\cdots(12)$$

where, $C_p{}^{N+1/2}$, $C_E{}^{N+1/2}$, and $C_W{}^{N+1/2}$ are the unknown parameters, and the others are the parameters known at time N. Using the result of $C_p{}^{N+1/2}$, the second half of the time step can be calculated from the following equation.

$$\{(\Sigma b+\Sigma A^C)+2\Delta x\Delta y/\Delta t\}C_p{}^{N+1/2}$$
$$=(b_E+A_E{}^C)C_E{}^{N+1/2}+(b_W+A_W{}^C)C_W{}^{N+1/2}$$
$$+(b_N+A_N{}^C)C_N{}^{N+1}+(b_S+A_S{}^C)C_S{}^{N+1}$$
$$+G_p\Delta x\Delta y+2\Delta x\Delta y C_p{}^{N+1/2}/\Delta t \qquad \cdots\cdots(13)$$

4. Calculation Method

4.1 Steady State

The basic room model is shown in **Figure 2.** Fresh air is supplied from the top center and the room air is exhausted from the right bottom. The

Table 1 Boundary conditions for numerical calculation

	ψ	ω	k	ε	C	ν
ABCD	0.0	*	0.0	0.0	**	0.0
DE	$\partial\psi/\partial x=0.0$	$\partial\omega/\partial x=0.0$	$\partial k/\partial x=0.0$	$\partial\varepsilon/\partial x=0.0$	**	$\partial\nu/\partial x=0.0$
EFG	1.0	*	0.0	0.0	**	0.0
GA	$\partial\psi/\partial x=1.0$	0.0	0.04	0.008	0.0	0.018

* $\left(\frac{\partial\omega}{\partial n}\right)_w = \frac{\omega_w-\omega_{w-1}}{\Delta n}$ ** $C_w=C_{w-1}$

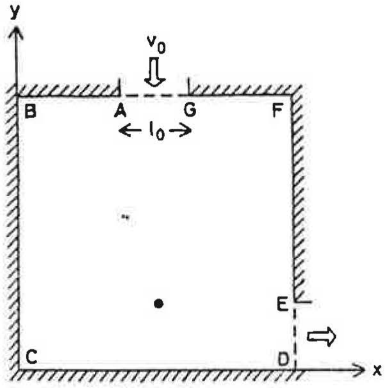

Fig.2 Basic room model(• shows the pollutant generation site)

Table 2 Constants used for numerical calculation

σ_μ	σ_1	σ_2	σ_k	σ_ε	σ_C
0.09	1.44	1.92	1.0	1.3	0.9

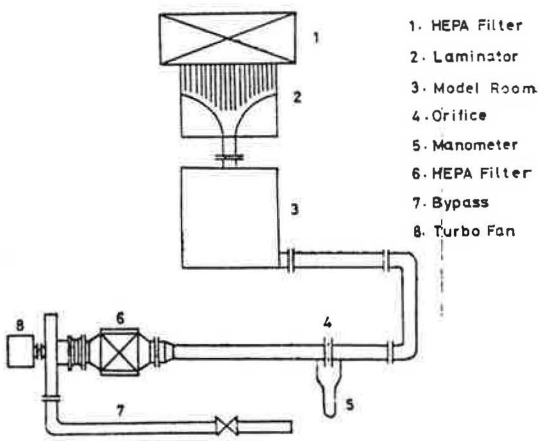

Fig.3 Schematic diagram of experimental setup

pollutant generation site was set at the center of the lower part. **Table 1** summarizes the boundary conditions for the calculation. The constants used in the turbulent flow model are shown in **Table 2**, and are the values recommended by Launder et al[4]. Equations (1) through (5) were solved simultaneously. Calculation was terminated when the maximum value of the relative change of each parameter at every point in the room,

$$\left|\frac{\phi^N-\phi^{N-1}}{\phi^N}\right|^{i,j}_{max} \quad ; \quad \phi=\psi, \omega, k, \varepsilon, C$$

became smaller than 1.0×10^{-4}.

4.2 Unsteady State

Since the change in concentration with time is rapid at first and is slow afterwards, time step Δt was made to increase in geometric ratio with the initial interval of 0.1 and the common ratio of 1.01.

5. Experimental Confirmation of the Results of Numerical Calculation

5.1 Method

Before making any conclusions from the results of the numerical calculation, its validity was examined experimentally. The experimental setup is shown schematically in **Figure 3**. The model room was made of a 40 cm acrylic cube. The width of the inlet and outlet slits was 4.0 cm. A laminator was attached above the inlet. The total flow rate was measured with an orifice. The velocity at each point in the model room was measured with a hot wire anemometer (Nihon Kagaku Kogyo Co., Ltd. Model 1010). Carbon monoxide gas was used as the pollutant. Its concentration was measured with a CO meter (GASTEC Co., Ltd. Model CM-2510).

5.2 Results

Typical results for the flow velocity in the x-direction, u, and y-direction, v, are presented in **Figure 4** by solid and open circles, respectively. The results of the corresponding numerical computation using equally spaced 20×20 mesh grids are shown by the solid and broken lines in the

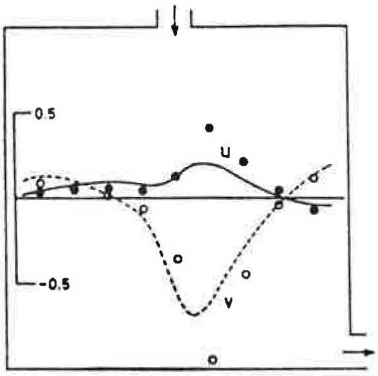

Fig. 4 Typical results of flow velocities in the model room at $y=20$ cm

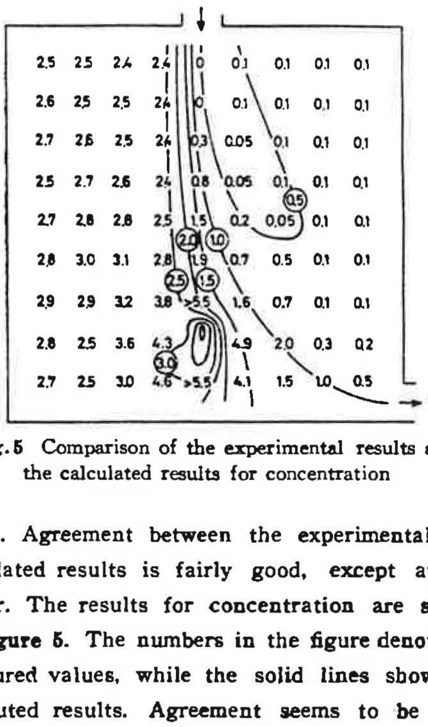

Fig. 5 Comparison of the experimental results and the calculated results for concentration

figure. Agreement between the experimental and calculated results is fairly good, except at the center. The results for concentration are shown in **Figure 5**. The numbers in the figure denote the measured values, while the solid lines show the computed results. Agreement seems to be good except in the low concentration region. As for concentration decay, the slope was about 10% steeper for the calculated results. These discrepancies seem to be mainly due to the rather coarse mesh grid used in the calculation. Allowing for these small discrepancies between the results of the numerical calculation and the experiments, it can be said that the k-ε model of turbulent flow presented here gives satisfactory expressions for the real flow pattern and concentration.

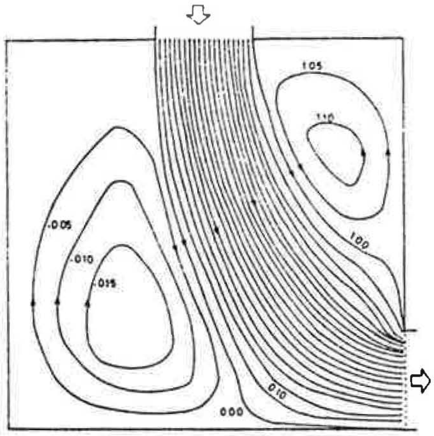

Fig. 6 Stream function when the inlet is at top center

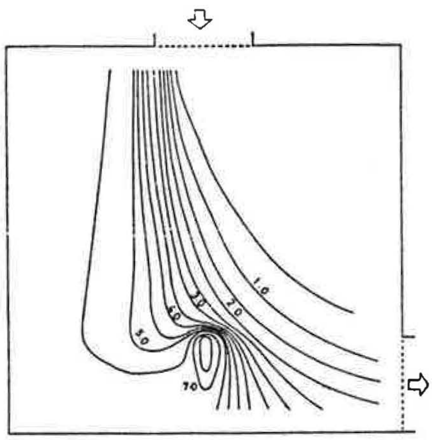

Fig. 7 Concentration when the inlet is at top center

6. Results of Numerical Calculation

To save CPU time, all of the following calculations, except for those for a wide room (32×16) and a high room (16×32), were performed in 16×16 equally spaced mesh grids.

6.1 Steady State

The stream function and concentration with a Reynolds number of 1.0×10^4 are shown in **Figures 6 and 7. Figure 6** shows that the most of the supplied air flows from the inlet through the outlet and some circulates at the corners. **Figure 7** shows that the concentration is very high at the pollutant generation site and its change is steep around the main part of the flow. **Figures 8 through 10** show the vorticity, turbulent flow energy, and dissipation rate of turbulent flow energy. It can be seen

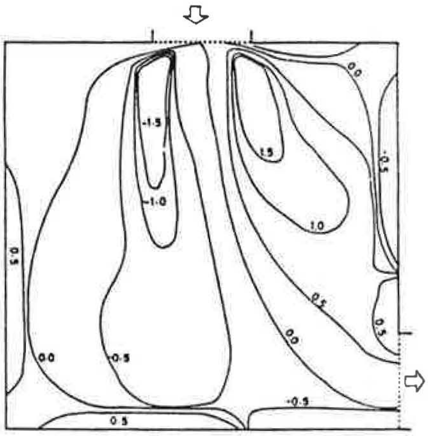

Fig. 8 Vorticity when the inlet is at top center

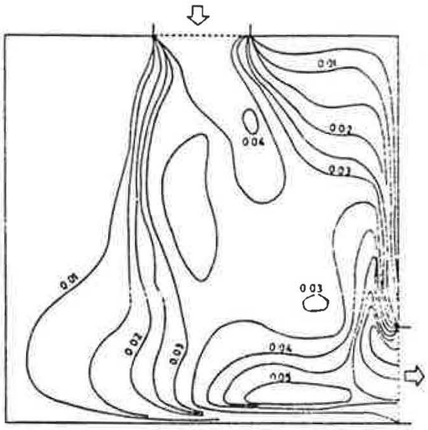

Fig. 9 Turbulence kinetic energy when the inlet is at top center

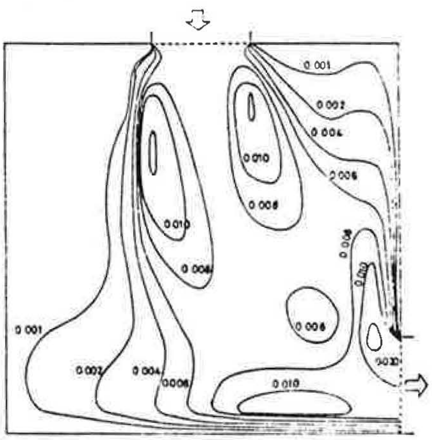

Fig. 10 Turbulence energy dissipation rate when the inlet is at top center

from **Figure** 8 that the vorticity is high near the inlet and the vortex motion is in the opposite direction between the right and left sides. The turbulent flow energy and its dissipation rate are

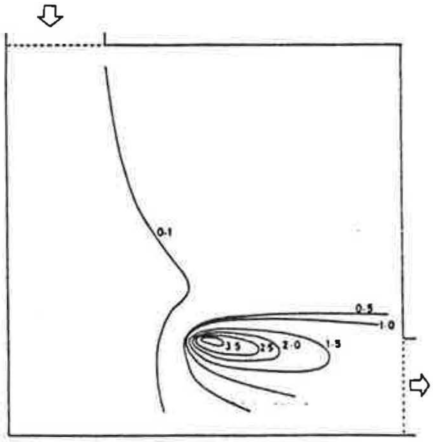

Fig. 11 Concentration when the inlet is at top left

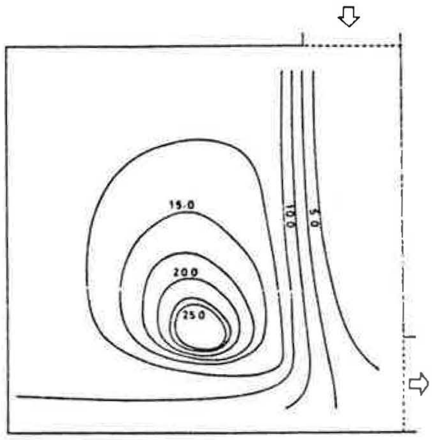

Fig. 12 Concentration when the inlet is at top right

high near the inlet and the outlet. The patterns of **Figures** 9 and 10 are similar, except near the inlet. **Figures** 11 and 12 show the concentration when the inlet position is changed to the top left and the top right, respectively. As shown in these figures, the average concentration becomes lower when the inlet is at the top left or, in other words, the flow pass length in the room becomes longer. **Figures** 13 and 14 show the concentration when the flow rate or Reynolds number is changed. As shown in these figures, there is little change in the concentration distribution. **Figures** 15 through 19 show the concentration for other inlet positions. **Figures** 20 and 21 show the concentration for different types of rooms. **Figures** 22 and 23 show the concentration for different pollutant generation sites. When the pollutant generation site is near the outlet, the pollutant is exhausted

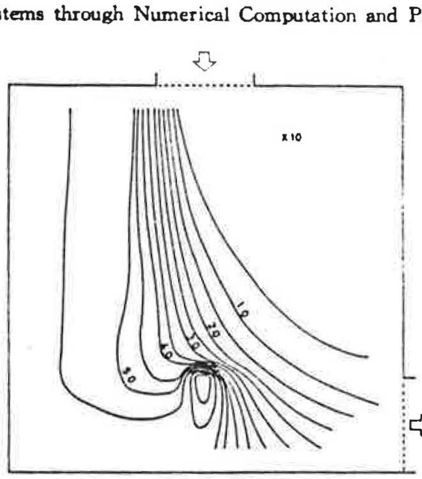

Fig. 13 Concentration when the Reynolds number is 1.0×10^3

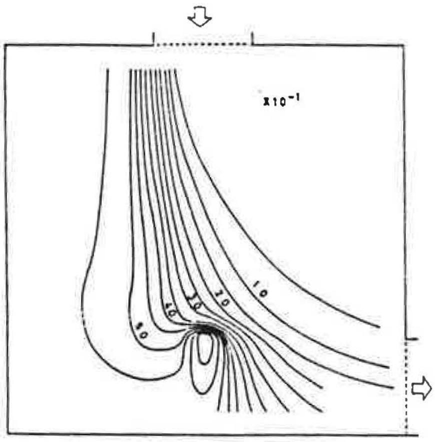

Fig. 14 Concentration when the Reynolds number is 1.0×10^5

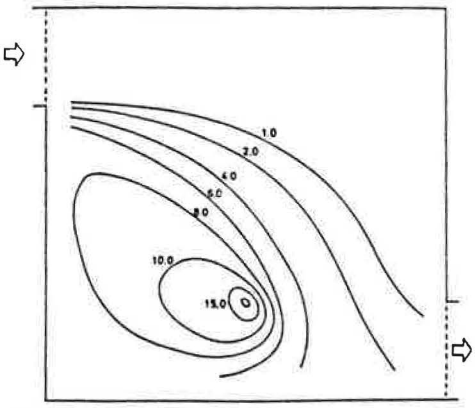

Fig. 15 Concentration when the inlet is at left top

before it diffuses in the room, thus resulting in a much lower concentration in the room.

6.2 Unsteady State

When pollutant generation stops, the concentra-

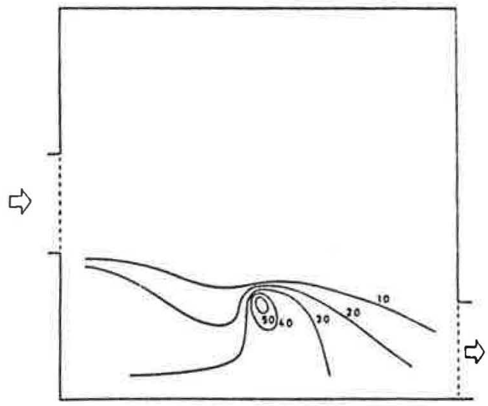

Fig. 16 Concentration when the inlet is at left center

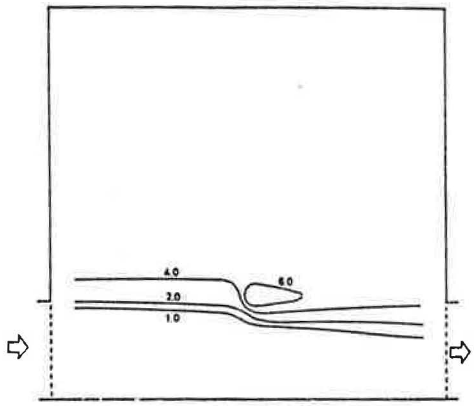

Fig. 17 Concentration when the inlet is at left bottom

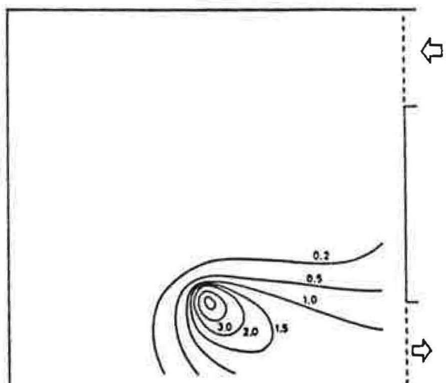

Fig. 18 Concentration when the inlet is at right top

tion decays. This decay has been plotted on a semi-logarithmic graph as shown in **Figure 24**. The slope of the concentration decay curve differs with the site for some time after the end of pollutant generation, but appears to remain virtually the same afterwards. Therefore, it seems to be very convenient to take this slope as an index of

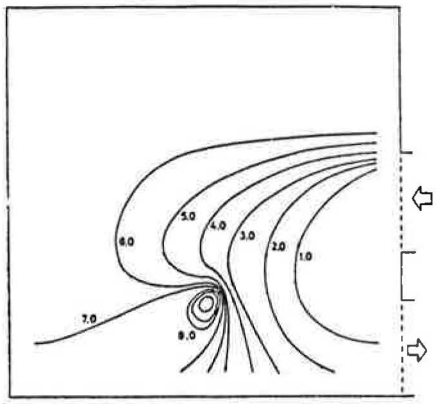

Fig. 19 Concentration when the inlet is at right center

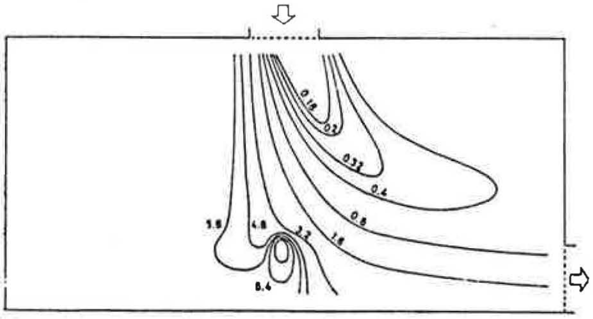

Fig. 20 Concentration when room is wide

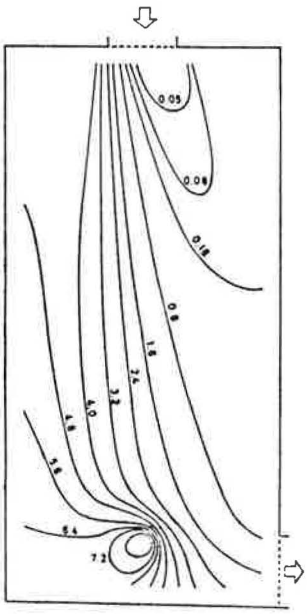

Fig. 21 Concentration when room is high

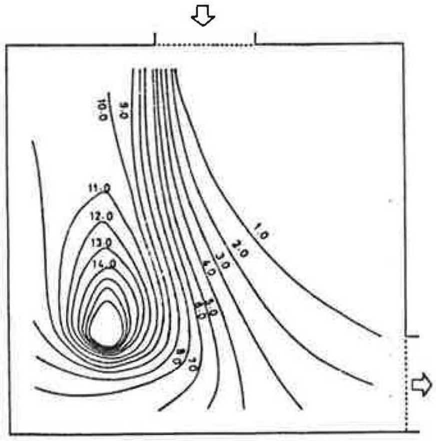

Fig. 22 Concentration when the pollutant generation site is at left of the lower part

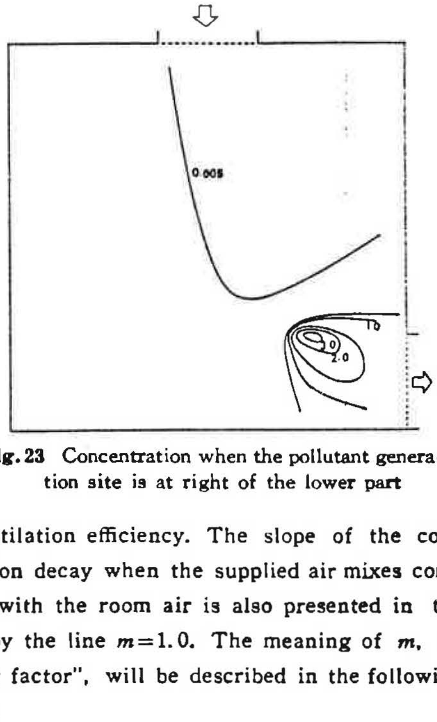

Fig. 23 Concentration when the pollutant generation site is at right of the lower part

the ventilation efficiency. The slope of the concentration decay when the supplied air mixes completely with the room air is also presented in the figure by the line $m=1.0$. The meaning of m, or "mixing factor", will be described in the following section.

Further, since the slope of the concentration decay curve seems to become virtually the same with the lapse of time regardless of the site in the room, the concentration distribution becomes constant. An example of this concentration distribution is presented in **Figure** 25.

The results presented here are those for two dimensional cases and are not directly applicable to actual three dimensional rooms in general, but are applicable qualitatively, at least.

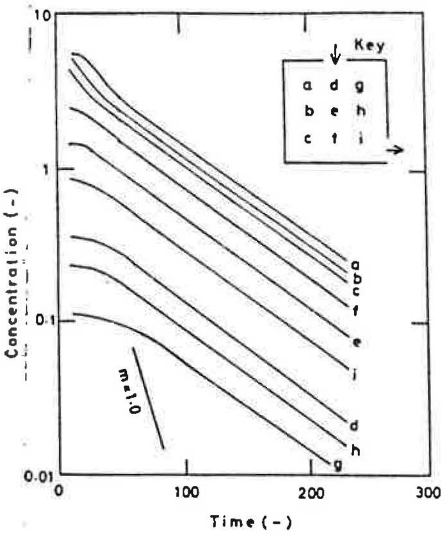

Fig. 24 Decay of concentration with time

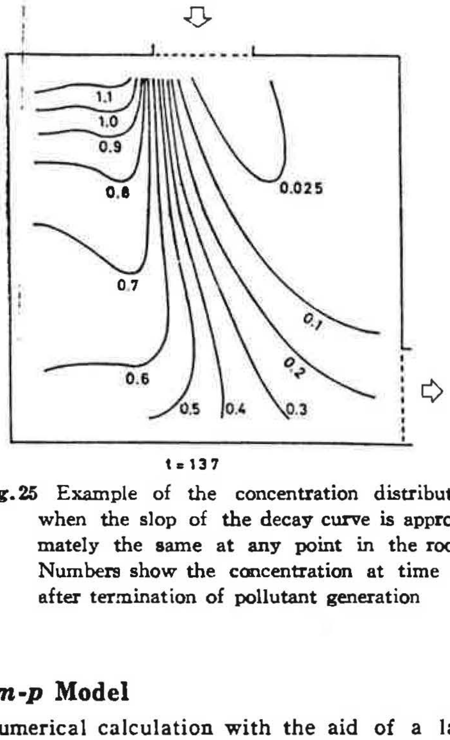

Fig. 25 Example of the concentration distribution when the slop of the decay curve is approximately the same at any point in the room. Numbers show the concentration at time 137 after termination of pollutant generation

7. *m-p* Model

Numerical calculation with the aid of a large-scale computer seems to be a preferable way of predicting the real state of indoor air pollution, or the distribution of the concentration of pollutants. However, this method is expensive and such computers are not always accessible. Accordingly, a simple equation by which a quantitative estimation of the concentration can be made is often preferable. For this purpose, a new ventilation model we tentatively call an *m-p* model is presented considering the mixing model used in the Chemical Engineering field.

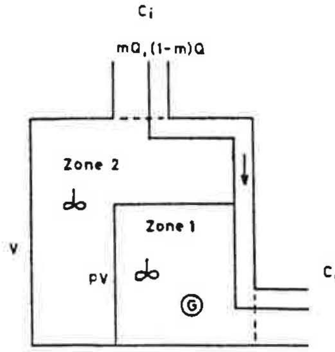

Fig. 26 Basic idea for *m-p* model

It seems to be a reasonable assumption that the main factors governing the pollutant concentration in a room with a fixed number of air changes are the ventilation efficiency and the pollutant generation site. As shown in **Figure 26**, it is assumed that the mQ portion of the supplied air mixes completely with the room air and the $(1-m)Q$ portion by-passes without mixing[5),6)]. We call m the "mixing factor". It is also assumed that the room is composed of two zones. Zone 1 is the region of volume pV where the pollutant diffuses completely. Zone 2 is the fresh air region of volume $(1-p)V$. We call p the "position factor". As a whole, the supplied air becomes Q, the pollutant generation rate becomes G, and the volume of the room becomes V. Then the average concentration for the whole room can be expressed as,

$$C=C_1V_1/V+C_2V_2/V=C_1p+C_2(1-p) \qquad \cdots\cdots(14)$$

The pollutant concentration in the exhaust air becomes,

$$C_e=C_1Q_1/Q+C_bQ_b/Q=C_1m+C_b(1-m) \qquad \cdots\cdots(15)$$

Here, subscript b represents by-pass. The volume of the by-pass region is assumed to be zero. Further, it is assumed that when no pollutant is generated, G is zero and p is unity. The pollutant concentration in Zone 1, C_1, can be expressed by the mass balance equation:

$$C_1-C_i=\left\{(C_0-C_i)-\frac{G}{mQ}\right\}\exp\left(-\frac{mQ}{pV}t\right)+\frac{G}{mQ} \qquad \cdots\cdots(16)$$

Letting time t go to infinity gives the steady

Table 3 m and p for various types of ventilation systems

Case	1	2	3	4	5	6	7	8	9	10	11	12
	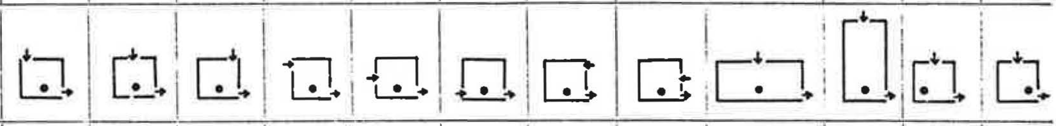											
m	0.42	0.22	0.11	0.39	0.21	0.08	0.77	0.14	0.20	0.27	0.22	0.22
p	0.12	0.63	1.1	1.5	0.16	0.31	0.19	0.72	0.66	0.71	1.1	0.03
p/m	0.29	2.9	10	3.7	0.76	3.9	0.25	5.1	3.3	2.6	5.0	0.14

● indicates the pollutant generation site

state concentration as follows:

$$C_1-C_i=\frac{G}{mQ} \qquad \cdots\cdots(17)$$

From Equations (14) and (17), the concentration for the whole room can be expressed as follows:

$$C=\left(C_i+\frac{G}{mQ}\right)p+C_i(1-p)=\frac{pG}{mQ}+C_i \qquad \cdots\cdots(18)$$

From Equations (15) and (17), the concentration in the exhaust air can be expressed by:

$$C_e=\left(C_i+\frac{G}{mQ}\right)m+C_i(1-m)=\frac{G}{Q}+C_i \qquad \cdots\cdots(19)$$

In this case, the effect of dividing the room into two zones does not appear and the concentration becomes a reasonable value of $G/Q+C_i$. This seems to support the validity of the model.

When pollutant generation ends, the concentration in Zone 1 can be expressed by making $G=0$ and $p=1.0$ in Equation (16). Thus,

$$C_1-C_i=(C_0-C_i)\exp\left(-\frac{mQ}{V}t\right) \qquad \cdots\cdots(20)$$

From Equations (14) and (20), the concentration for the whole room with the lapse of time becomes C_i. The concentration decay in the exhaust air can be expressed from Equations (15) and (20) as,

$$C_e-C_i=m(C_0-C_i)\exp\left(-\frac{mQ}{V}t\right) \qquad \cdots\cdots(21)$$

From this equation, the total amount of pollutant exhausted becomes,

$$\int_0^{\infty} Q(C_e-C_i)dt=(C_0-C_i)V \qquad \cdots\cdots(22)$$

and this is the total amount of pollutant existed

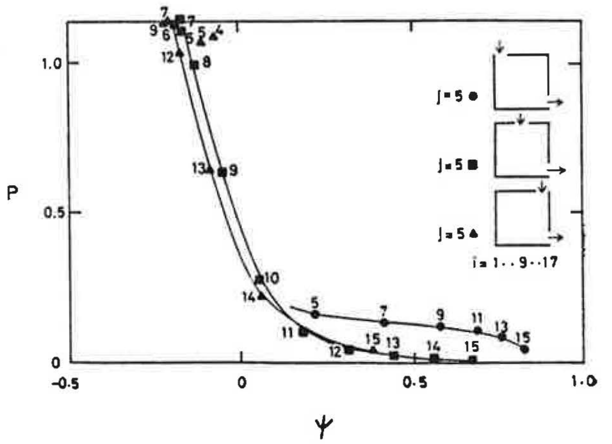

Fig. 27 Relation between ψ and p when the pollutant generation site is changed in the x-direction with a fixed height for three types of ventilation

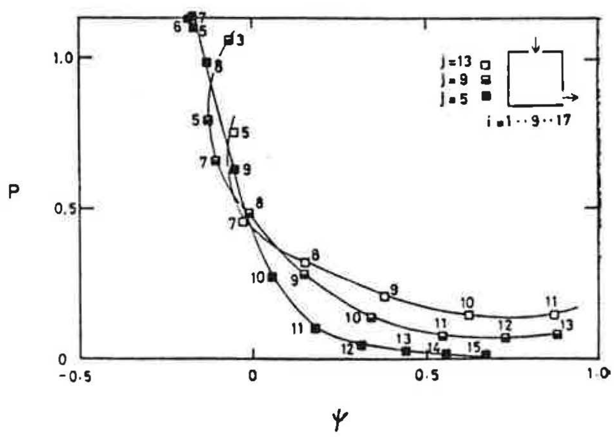

Fig. 28 Relation between ψ and p when the pollutant generation site is changed in the x-direction with three levels of fixed height

in the room. This reasonable result also seems to support the validity of the m-p model.

From these considerations, the average concentration of pollutant in indoor spaces can be suitably expressed by applying m, or mixing factor and p, or position factor.

Now, we try to link these factors to the results of numerical calculations. Let the steady state concentration at site (i, j) in the room be $C_\infty^{i,j}$, which can be obtained from the results of numerical calculation for each ventilation system. Then the average steady state concentration in the room, C_∞, can be calculated from $\sum\sum C_\infty^{i,j}/(i\times j)$. The mixing factor at site (i, j) in the room, $m^{i,j}$, can also be obtained from the results of the concentration decay of the numerical calculation. As previously described, $m^{i,j}$ seems to become virtually the same value m with the lapse of time, regardless of the position in the room. Thus the value m can be taken as the average mixing factor of the room. Corresponding to Equation (18), we define the average position factor p by the equation $C_\infty=p/m$. Then p can be derived from the values C_∞ and m described above. All of these values in each ventilation system are summarized in **Table 3**. It is apparent from **Table 3** that the flow pattern, which is mainly governed by the geometry of the room, determines the mixing factor m and that the pollutant generation site is irrelevant to m. Effective ventilations of larger m can be obtained when the supplied air pass length in a room is longer, like cases 7, 1, and 4. The position factor p is more complicated, but it seems to depend mainly on the value of the stream function at the pollutant generation site as shown in **Figures** 27 and 28. If the pollutant generation site is near the outlet, p becomes extremely small, like case 12 in **Table 3**.

In applying this model to actual rooms, it seems easy and adequate to measure the values of m and p by experiment beforehand. The values of m can be derived by measuring the concentration decay and p can be derived from the relation $C_\infty=p/m$ by measuring the average steady state concentration of the room.

Since the average concentration is proportional to p/m, to make p small and/or to make m large can be a criterion for effective cleaning of the indoor air pollutants with a fixed number of air changes.

8. Conclusion

1) After the termination of pollutant generation, the slope of the concentration decay seems to approach a certain value with the lapse of time regardless of the position in a room. Thus it seems very convenient to take this slope as an indicator of the ventilation efficiency.

2) Ventilation efficiency is higher when the main flow pass length of the supplied air is longer in the room.

3) A new ventilation model which permits quantitative estimation of the concentration with simple manipulation is proposed. The model includes two new parameters; "mixing factor" m showing the ventilation efficiency and "position factor" p showing the effect of the pollutant generation site on the average concentration.

4) Making p small and/or making m large can be a criterion for effective cleaning of the indoor air with a fixed number of air changes.

References

1) I. Tani: Turbulent Flow, (1980), Maruzen Co., Ltd, Tokyo (in Japanese)
2) B.E. Launder and D.B. Spaulding: Mathematical Models of Turbulence, (1972), Academic Press, London
3) K. Yamaguchi, Y. Inoue, K. Yoneyama, and A. Yoshikawa: Numerical Solution of Room Air Distribution (Part 5) Calculation and Experiment of Two-Dimensional Turbulent Room Air Distribution (1), Trans. SHASE (The Society of Heating, Air-Conditioning and Sanitary Engineers of Japan), No.6 (1978), pp.75~84
4) B.E. Launder and D.B. Spaulding: The Numerical Computation of Turbulent Flows, Comp. Method Appl. Mech. Engr., 3(1974), pp.269~289
5) N.A. Esmen: Characterization of Contaminant Concentration in Enclosed Spaces, Environ. Sci. Technol., 12(1978), pp.337~339
6) Y. Ishizu: General Equation for the Estimation of Indoor Pollution, Environ. Sci. Technol., 14(1980), pp.1254~1257

(Received April 25, 1983)